Structure, Vol. 9, 1143–1152, December, 2001, ©2001 Elsevier Science Ltd. All rights reserved. PII S0969-2126(01)00679-7

The Structure of Phosphorylated GSK-3β Complexed with a Peptide, FRATtide, that Inhibits β-Catenin Phosphorylation

Benjamin Bax,[1,8] Paul S. Carter,[2] Ceri Lewis,[2] Angela R. Guy,[3] Angela Bridges,[3] Robert Tanner,[4] Gary Pettman,[4] Chris Mannix,[4] Ainsley A. Culbert,[5] Murray J.B. Brown,[6] David G. Smith,[7] and Alastair D. Reith[6]

[1] Departments of Structural Biology
[2] Department of Protein Biochemistry
[3] Department of Gene Expression Sciences
[4] Department of Microbial and Cell Culture Sciences
[5] Neurology Centre of Excellence in Drug Discovery
[6] Systems Research, and
[7] Department of Medicinal Chemistry
GlaxoSmithKline Pharmaceuticals
Harlow, Essex CM19 5AD
United Kingdom

Summary

Background: Glycogen synthase kinase-3 (GSK-3) sequentially phosphorylates four serine residues on glycogen synthase (GS), in the sequence SxxxSxxxSxxx-SxxxS(p), by recognizing and phosphorylating the first serine in the sequence motif SxxxS(P) (where S(p) represents a phosphoserine). FRATtide (a peptide derived from a GSK-3 binding protein) binds to GSK-3 and blocks GSK-3 from interacting with Axin. This inhibits the Axin-dependent phosphorylation of β-catenin by GSK-3.

Results: Structures of uncomplexed Tyr216 phosphorylated GSK-3β and of its complex with a peptide and a sulfate ion both show the activation loop adopting a conformation similar to that in the phosphorylated and active forms of the related kinases CDK2 and ERK2. The sulfate ion, adjacent to Val214 on the activation loop, represents the binding site for the phosphoserine residue on 'primed' substrates. The peptide FRATtide forms a helix-turn-helix motif in binding to the C-terminal lobe of the kinase domain; the FRATtide binding site is close to, but does not obstruct, the substrate binding channel of GSK-3. FRATtide (and FRAT1) does not inhibit the activity of GSK-3 toward GS.

Conclusions: The Axin binding site on GSK-3 presumably overlaps with that for FRATtide; its proximity to the active site explains how Axin may act as a scaffold protein promoting β-catenin phosphorylation. Tyrosine 216 phosphorylation can induce an active conformation in the activation loop. Pre-phosphorylated substrate peptides can be modeled into the active site of the enzyme, with the P1 residue occupying a pocket partially formed by phosphotyrosine 216 and the P4 phosphoserine occupying the 'primed' binding site.

[8] Correspondence: benjamin_d_bax@gsk.com

Introduction

Glycogen synthase kinase-3 (GSK-3) is a ubiquitously expressed serine/threonine kinase that was originally discovered and named as a kinase that phosphorylates and inactivates glycogen synthase (GS) [1]. However, because GSK-3 has subsequently been shown to phosphorylate a wide range of cellular proteins, its activity is thought to be important not only to the regulation of glycogen synthesis, but also to multiple cellular processes [2]. The two mammalian isoforms of GSK-3, GSK-3α and GSK-3β, share a sequence identity of some 95% in the catalytic domain. Although more divergent at the amino and carboxy termini, both posses a serine residue near the N terminus, the phosphorylation of which is important to the regulation of GSK-3 activity. In resting cells, GSK-3 is highly active, but its activity can be inhibited physiologically in response to insulin and/or growth factor stimulation of a relatively well-characterized PI3 kinase-dependent signal transduction pathway [3]. Protein kinase B (PKB) lies on this pathway and is responsible for the direct phosphorylation of GSK-3 on an N-terminal serine residue (residue 9 in GSK-3β and serine 21 in GSK-3α), leading to inhibition of GSK-3 toward its substrates, such as GS. Consequently, the phosphorylation and inactivation of GS is prevented, contributing to a stimulation of glycogen synthesis [3–5]. Substrates of GSK-3, such as GS, that contain a "priming" phosphate located at n + 4 (where n is the site of phosphorylation) are phosphorylated more readily than substrates that lack a priming site. When phosphorylated on serine 9, the N-terminal residues of GSK-3β inhibit the enzyme by binding in the active site as a pseudo-substrate [6], with residue proline 5 presumably blocking the active site. Interestingly, a phosphopeptide (TTSpFAESC) corresponding to residues 7–14 of GSK-3β inhibits GSK-3 activity against primed, but not against nonprimed, substrates [6].

GSK-3 activity can also be inhibited in response to Wnt growth factor signaling. Wnt molecules control numerous developmental processes by altering specific gene expression patterns [7], and deregulation of Wnt signaling can lead to cancer [8, 9]. Cytoplasmic β-catenin is central to the transmission of Wnt signals to the nucleus; in the absence of Wnt signaling, β-catenin is phosphorylated by GSK-3, which targets β-catenin for degradation via ubiquitin-dependent proteolysis. In response to Wnt signals, however, GSK-3 activity toward β-catenin is inhibited, resulting in the stabilization and accumulation of β-catenin and the activation of TCF/LEF-1 transcription factors. The exact mechanisms by which Wnt signals inhibit GSK-3 activity toward β-catenin are unclear, but they involve the regulation of a signaling complex that consists of, among other proteins, GSK-3, Dvl, Axin, APC, and β-catenin. Genetic studies have shown that Dvl, a cytoplasmic protein downstream of Wnt receptors, is

Key words: Kinase structure; GSK-3; kinase phosphorylation; protein-protein interactions; FRAT; Axin

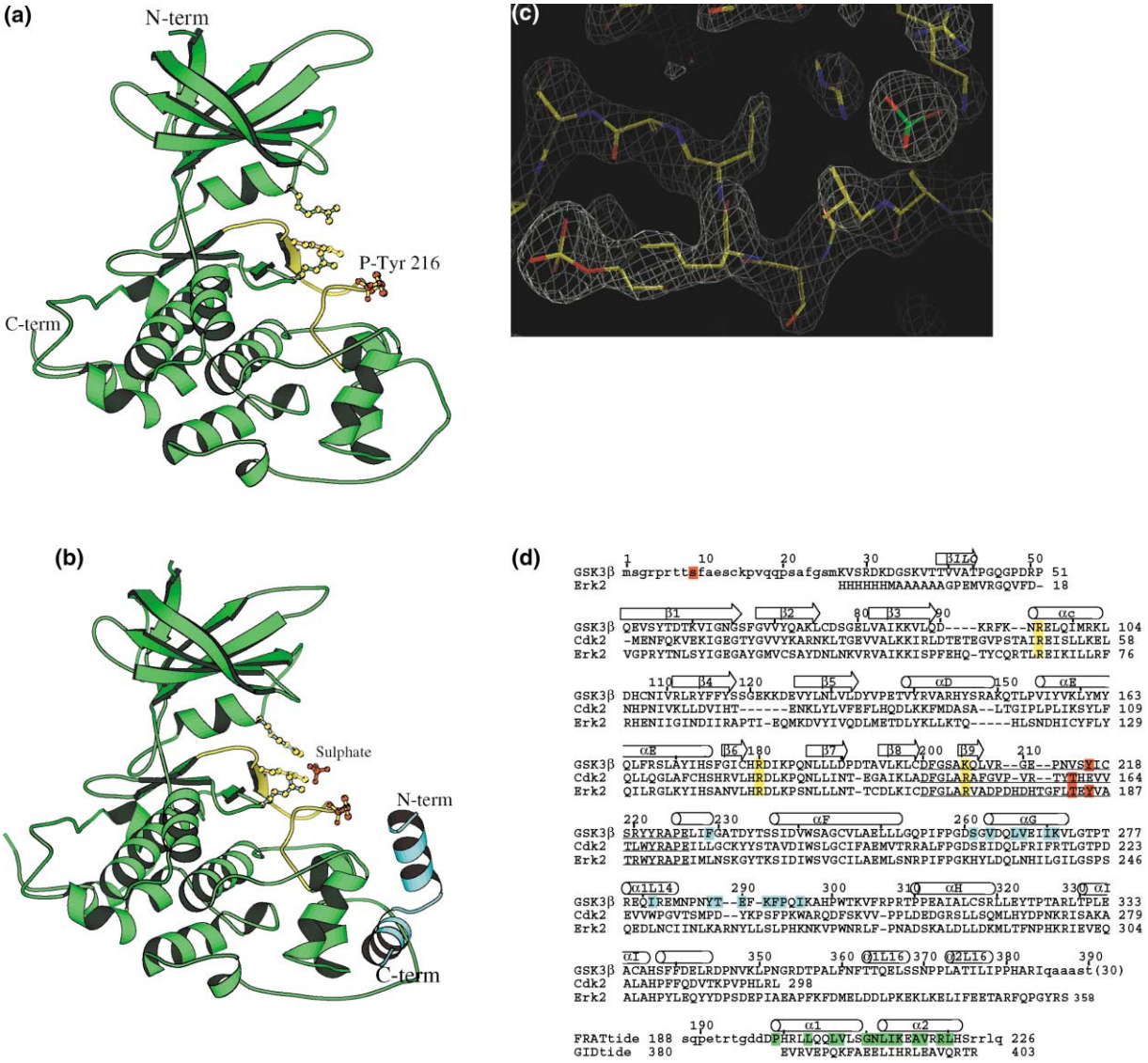

Figure 1. Structure of GSK-3

(a) Structure of crystal form A of GSK-3β. Phosphotyrosine 216 (red atoms) is labeled. The activation loop is in yellow, and the side chains of Arg 96, Arg 180, and Lys 205 are shown (yellow atoms).

(b) Structure of crystal form FS of GSK-3β. The FRATtide peptide is in blue, and the sulfate ion is in red ([a] and [b] were drawn with Bobscript [46]).

(c) Final $2F_o - F_c$ density (1.5 σ) of the FS crystal form showing the activation loop in the region of phosphotyrosine 216 and Val 214 and the sulfate ion adjacent to Val 214.

(d) Sequence alignment of GSK-3 with CDK2 and ERK2 (and FRATtide with the Axin-derived peptide GID underneath). GSK-3β (and FRATtide) residues in lowercase are not observed in the crystal structures reported in this paper. Secondary-structural elements in GSK-3 are indicated above the alignment. Residues highlighted in red are phosphorylation sites in the activation loop (and serine 9 at the N terminus of GSK-3β). The conserved basic residues highlighted in yellow contact the phosphothreonine residue in CDK2 and ERK2 but contact a sulfate ion in our crystal structure of GSK-3. Residues on GSK-3β that contact FRATtide (within 3.8 Å) are highlighted in blue, whereas residues on the FRATtide peptide that contact GSK-3 are highlighted in green.

essential for transmitting Wnt signals to GSK-3. Axin interacts with Dvl and, in addition, binds both GSK-3 and β-catenin. Axin facilitates GSK-3-mediated phosphorylation of β-catenin by bringing GSK-3 and β-catenin into close proximity [10–13]. Consequently, dissociation of the GSK-3/Axin/β-catenin complex prevents GSK-3-mediated phosphorylation of β-catenin, resulting in its stabilization. One proposed mechanism for Wnt-induced dissociation of the GSK-3/Axin/β-catenin complex involves the mammalian protein FRAT1 [14]. FRAT1 is homologous to GSK-3 binding protein (GBP), a protein identified in *Xenopus* embryos that acts as a positive regulator of Wnt signaling by stabilizing β-catenin [15]. In Wnt signaling, Dvl may recruit FRAT1 to the GSK-3/Axin/β-catenin complex and cause a FRAT1-mediated dissociation of GSK-3 from Axin [16]. Since Axin is a substrate of GSK-3, dissociation of Axin from GSK-3 would tend to result in the

dephosphorylation of Axin [17]. The Wnt-induced dephosphorylation of Axin decreases the affinity of Axin for β-catenin and allows β-catenin to be released from the GSK-3/Axin/β-catenin complex [18].

In vitro studies of a 39 residue peptide from the C terminus of FRAT1, termed FRATtide, have shown that this peptide binds GSK-3 and is sufficient for preventing Axin binding [19]. Consequently, FRATtide inhibited the phosphorylation of Axin and β-catenin, but it did not inhibit GSK-3 activity toward peptides derived from eIF2B or GS [19]. A 25 amino acid sequence in Axin, identified as a GSK-3-interacting domain (GID), inhibits GSK-3β and activates Wnt signaling [20]. This Axin-derived GID peptide did not inhibit activity, in vitro, toward a GS-derived peptide [20]. Although the GID and FRATtide peptides have a similar functionality, the GSK-3 binding domains in FRAT and Axin do not appear to have homologous amino acid sequences.

This paper describes the crystal structures of isolated tyrosine 216-phosphorylated GSK-3β and of a complex of GSK-3β with FRATtide and a sulfate ion. The sulfate ion binds at what is the binding site for the priming phosphorylation in substrate peptides, and in recent crystal structures of unphosphorylated GSK-3β, a phosphate [21] or a sulphonate [22] has been observed at this site. Phosphorylation of the activation loop is a common regulatory feature of protein kinases [23], and the phosphotyrosine 216 form of the enzyme shows the active conformation of the enzyme, allowing a substrate peptide to be modeled into the active site. The structure with FRATtide identifies a novel binding site, on the kinase domain's C-terminal lobe, at which FRAT and Axin compete for binding to GSK-3. This provides a structural explanation as to why FRATtide inhibits the phosphorylation of Axin and β-catenin, but not primed substrates [19]. Small-molecule ATP-competitive inhibitors of GSK-3 have potential therapeutic use in disease states associated with elevated GSK-3 activity; such disease states include non-insulin-dependent diabetes mellitus and neurodegenerative diseases [24, 25]. Such inhibitors are likely to inhibit GSK-3 activity toward all cellular substrates. Protein inhibitors such as FRAT, which appear to regulate kinase activity by modulating protein interactions within signaling complexes, may well inhibit activity toward a selected subset of substrates and may be the target for structure-based ligand design.

Results

The Overall Structure of Tyrosine 216-Phosphorylated GSK-3β

The crystal structures of apo GSK-3β (crystal form A) and of GSK-3β complexed with the 39mer peptide FRATtide and a sulphate ion (crystal form FS) were determined and refined to 2.9 Å and 2.6 Å, respectively (see Experimental Procedures for details). The crystallized protein was expressed in baculovirus from an N-terminally deca-His-tagged construct corresponding to residues 27–393 of human GSK-3β and was phosphorylated on tyrosine 216 in the activation loop.

The overall structure of GSK-3β (shown in Figure 1) is similar to that of other protein kinases. CDK2 and ERK2 are the most closely related Ser/Thr kinases whose structures have been determined. GSK-3β shares some 33% amino acid sequence identity with both CDK2 and the MAP kinase ERK2 over the core kinase domain (residues 55–345 of GSK-3β, as in Figure 1d), although phylogenetic analysis suggests GSK-3 is more closely related to the MAP kinase ERK2 than to CDK2 [26]. The core of the kinase domain is elaborated in GSK-3 by unique structural elements at the N and C termini. At the N terminus a unique β strand, β_{LO}, (residues Thr 38–Thr 43) forms a β hairpin with an extended β1 β strand (residues 38–42 hydrogen bond to residues 52–56) while Thr 43 (from β_{L0}) forms two main-chain hydrogen bonds with Phe 115 (on β4). (Note that secondary-structural elements are named as in cAMP kinase, with additional elements named after the loop in which they are found). In one molecule of GSK-3β, the N-terminal residue is Ser 29, but in the other three molecules the first residue for which clear density is observed is Val 37 (in each crystal form there are two molecules in the asymmetric unit—our construct starts at residue 27—prior to which is a deca-His tag for which density is not observed). The C terminus of GSK-3β has a unique conformation from residue 343 onward; this starts with a somewhat irregular 3_{10} helix (338–344), includes a β turn (350–353), a short α helix (363–368), and another α helix (373–378) capped at the N terminus by a turn of 3_{10} helix (370–373). The last residue for which interpretable density is observed is Ile 384 (our construct terminates at asparagine 393).

A comparison of the two crystal forms shows that the phosphorylated GSK-3β has a very similar conformation in both crystal forms. However, major differences are seen in the loop between residues 285 and 310, with which the FRATtide peptide makes a number of interactions (see below for details). The small differences in the relative orientations of the N- and C-terminal domains of GSK-3 (rotations of less than 5° about the inter-domain connecting peptide) do not effect inter-domain contacts (the differences in domain orientation are of the same order between molecules in the two different crystal forms as they are between the two molecules in the same asymmetric unit of each crystal form). Some of the loops between secondary-structural elements in the N-terminal domain have high temperature factors and appear quite flexible. The conformation of the activation loop (200–226) is very similar in both crystal forms of GSK-3β; this includes the primed phosphate's binding pocket, which contains a sulfate ion in crystal form FS (grown from ammonium sulfate), but only a water (or hydroxide ion?) in crystal form A (grown from PEG at pH 8.2; see Experimental Procedures).

Conformation of the Activation Loop: Implications for Substrate Binding

In both crystal forms, the activation loop of GSK-3β has a conformation similar to that observed in active forms of ERK2 [27] and CDK2 [28]. The phosphate moiety of phosphotyrosine 216 of GSK-3 makes interactions with arginines 220 and 223. TyrP 216 in GSK-3 occupies a similar position to phosphotyrosine 185 in the MAP kinase ERK2, but in GSK-3 it is some 1.5 Å farther away

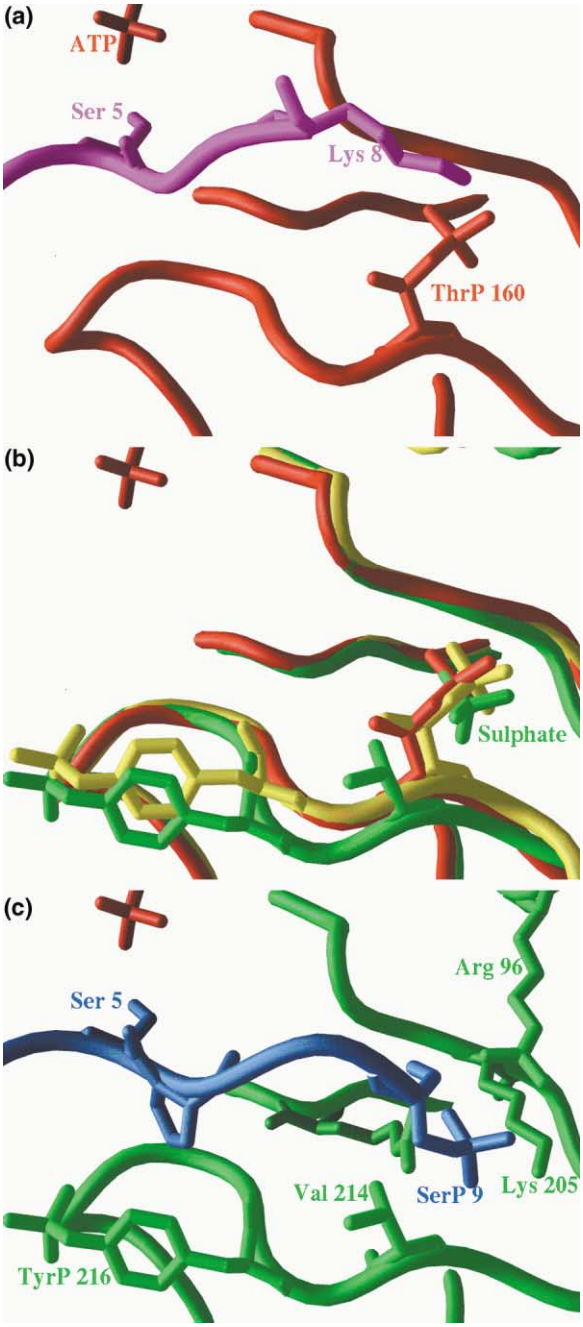

Figure 2. The Activation Loop and Substrate Binding

(a) The structure of CDK2 (red) with a substrate peptide (purple) and a nonhydrolizable analog of ATP (labeled ATP; only the terminal phosphate group is visible; PDB code 1QMZ; [28]). Ser 5 is the phosphorylatable serine in the substrate. Lysine 8 from the substrate peptide interacts with phosphothreonine 160.

(b) Superposed structures of CDK2 (red), ERK2 (yellow; PDB code 2ERK; [27]) and GSK-3 (green; FS crystal form). The sulfate in GSK-3 is labeled and superposes on phosphothreonine residues in CDK2 and ERK2.

(c) Coordinates of GSK-3 (green) are shown with a substrate peptide (blue) modeled in the active site. The peptide has been modeled on the peptide in the CDK2 crystal structure (a) with the phosphothreonine residue at position 9 modeled with its phosphate group occupying the position occupied by the sulfate in the crystal structure of the FS crystal form of GSK-3. The figure was drawn with GRASP [47].

from the substrate binding groove than TyrP 185 in ERK2 (Figure 2). This fact partially accounts for the wider substrate specificity of GSK-3 at the P1 position (tyrosine 216 in GSK-3 forms part of the binding pocket for the P1 residue of the substrate - see below). The phosphorylation of tyrosine 216 in GSK-3 is important for activity [29, 30] and presumably helps stabilize the activation loop in an active conformation.

In the FS crystal form (crystallized from 1.6 M ammonium sulfate), we see a sulfate ion adjacent to Val 214 (Figure 1c). This sulfate ion makes hydrogen bonds to three basic residues, arginines 96 and 180 and lysine 205. These three residues are conserved as basic residues in CDK2 and ERK2 where, in crystal structures of active forms of these proteins, they interact with a phosphothreonine residue on the activation loop. This residue is Thr 160 in CDK2 [28] and Thr 183 in ERK2 [27] (see Figure 2). Many GSK-3 substrates require a priming phosphorylation on a serine residue four residues C-terminal to the phosphorylatable serine or threonine residue. The binding site for this preexisting phosphate moiety on primed substrates is probably represented by the sulfate ion. Frame et al., 2001 [6] have shown that an Arg96Ala mutant of GSK-3β has a severely impaired ability to phosphorylate primed substrates and that this mutant is resistant to inhibition by phosphorylation on Ser 9.

A primed substrate peptide from GS (sequence RHSSPHQSp, where Sp represents a phosphoserine and S is the phosphorylatable residue) was modeled into the active site of GSK-3 (Figure 2; see Experimental Procedures for details). The terminal phosphoserine residue of this substrate peptide was positioned so that its phosphate moiety occupied the same position as the sulfate ion in the FS crystal form and was thus coordinated by arginines 96 and 180 and lysine 205. The proline residue at the P1 position of the substrate peptide occupied a depression partially formed by the aromatic ring of phosphotyrosine 216, but this P1 pocket is more open in GSK-3 than in the MAP kinase ERK2 because the phosphotyrosine 216 has moved down and away from the substrate (compared to phosphotyrosine 185 in ERK2). ERK2 has a strong preference for proline residues at the P1 position, whereas GSK-3 substrates have a wider range of P1 residues. The modeled substrate peptide made few other specific contacts (apart from the contacts of the phosphorylatable serine to Asp 181 and Lys 183).

The substrate binding groove, between the two lobes of the kinase domain, is above (in Figure 3a) the FRATtide binding site, so that there is no steric clash between a modeled substrate and the FRATtide.

The FRATtide Binding Site Is on the C-Terminal Lobe

In the crystal structure of the GSK-3β with FRATtide (a peptide that corresponds to residues 188–226 of the GSK-3 binding protein FRAT1), electron density is observed for residues 198–222 of the peptide (other FRATtide residues are disordered). The FRATtide comprises two α helices (α1 and α2), which form a helix-turn-helix motif that packs against the C-terminal lobe of GSK-3

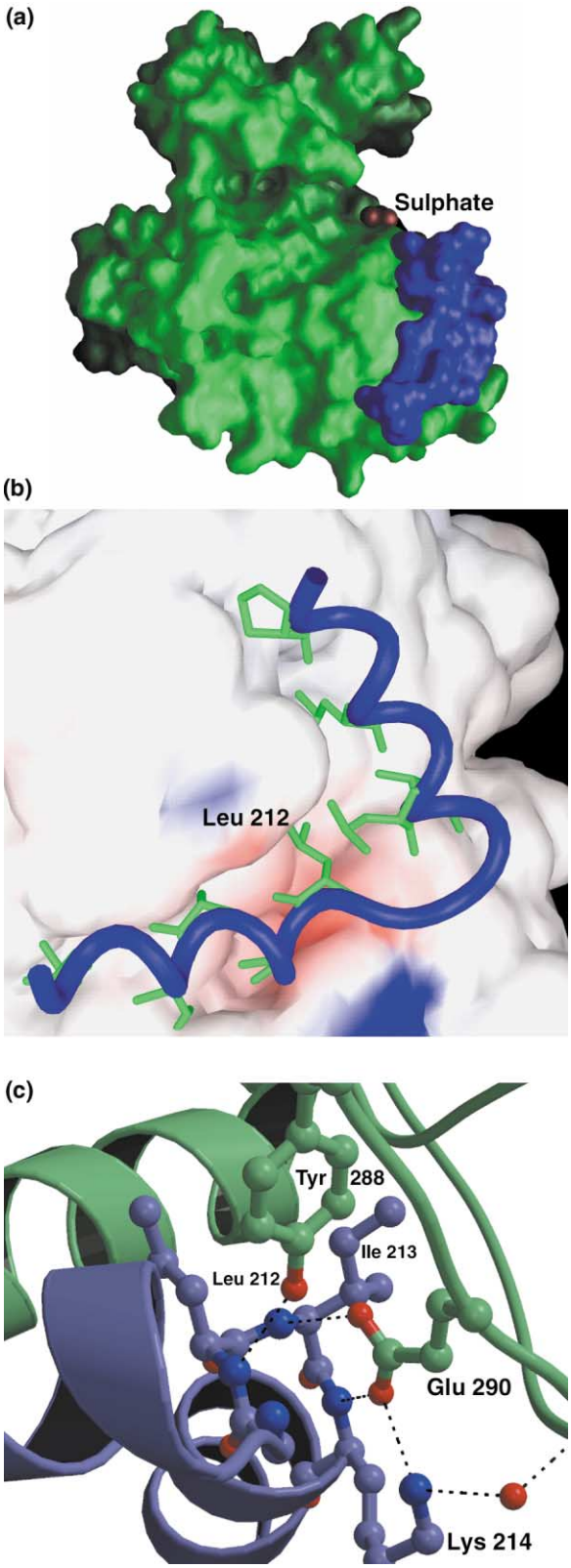

Figure 3. The GSK-3/FRATtide Interaction

(a) Surface representation of the structure of GSK-3 (green), FRATtide (blue), and the sulfate ion (red). The N terminus of the FRATtide approaches the sulfate ion (and the substrate binding groove). The C terminus of FRATtide is toward the bottom of the picture.

(b) The FRATtide peptide is shown with its backbone represented as a blue worm and hydrophobic side-chains contacting GSK-3 in green. The amino terminus of the FRATtide peptide (Asp 198) is toward the top of the figure. GSK-3 is represented as a solid surface, with negative electrostatic potential (red) due to Glu 288 from GSK-3 adjacent to the N terminus of the second helix of FRATtide.

(c) Hydrogen bonds (dotted lines) between Tyr 288 and Glu 300 from GSK-3 (green) and the residues Leu 212, Ile 213, and Lys 214 from FRATtide (blue). Hydrogen bonds from Lys 214 of FRATtide to a water and thence to the backbone of GSK-3 are also shown.

(Figures 1 and 3). The binding of FRATtide causes a change in the position of residues 286–296 of GSK-3. In crystal form A (without FRATtide), residues 286–296 pack close to and partially cover phenylalanine 229 and the hydrophobic surface of helix G (the 286–296 loop has high temperature factors in crystal form A, suggesting that the packing of Phe 291, Phe 293, and other residues against helix G is not optimal). Upon binding, FRATtide residues 288–294 of GSK-3 move approximately 6 Å away from helix G and open up a hydrophobic groove, between helix G and the 288–294 loop. The second, amphipathic, α2 helix of FRATtide slots neatly into this groove (FRATtide residues that interact with GSK-3 are highlighted in green on the sequence alignment in Figure 1d, whereas GSK-3 residues that interact with FRATtide are highlighted in blue; note that Lys 271 of GSK-3 makes van der Waals interactions with FRATtide via hydrophobic parts of its side chain). The first helix of FRATtide, α1, is also amphipathic but is less buried in packing against a flatter part of the surface of GSK-3. The N-terminal end of this α1 helix has higher temperature factors than the rest of FRATtide and, at His 200, comes quite close (approximately 4.3 Å) to the side chain of phosphotyrosine 216 in the activation loop of GSK-3.

Although much of the interaction of FRATtide with GSK-3 is mediated by hydrophobic interactions, an exquisite network of hydrogen bonds is formed to the N-terminal residues of the α2 helix of FRATtide (Figure 3). The side-chain functions of Tyr 288 and Glu 290 from GSK-3 make hydrogen bonds with the main-chain amides of Leu 212, Ile 213, and Lys 214 from FRATtide at the N terminus of α2. The side-chain nitrogen function of Lys 214 from FRATtide also interacts with Glu 290 from GSK-3 and, via a water molecule, with the main chain. The N-terminal leucine and isoleucine from the α2 helix of FRATtide are deeply buried in GSK-3 and, with the neighboring Lys and Glu in the sequence LIKE, appear to be a major determinant of FRAT binding to GSK-3 ([15]; see discussion below).

The Axin-derived GSK-3 binding peptide GID [20] also possesses a Leu-Ile sequence and is aligned with FRATtide on this basis in Figure 1d. Smalley et al., 1999 [12] found that mutation of this leucine residue in mouse Axin abolished binding to GSK-3.

An Axin-Derived Peptide Competes for the FRATtide Binding Site on GSK-3

The Axin-derived peptide called GID can compete with FRATtide for binding to GSK-3—although it binds with lower affinity ($K_d = 3.2 \pm 1.1$ μM, cf FRATtide $K_d = 39 \pm 7$ nM; Culbert et al., 2001 [31]). Presumably, GID binds

Table 1. TAMRA-FRATtide Ligand Displacement Assay

GID	K_d (μM)
WT	3.2 $\pm$ 1.1
L396M	12 $\pm$ 4
L392P	>>100
L392M	33 $\pm$ 8

to the same site on GSK-3 as FRATtide. Although the sequence of GID has little sequence identity to FRATtide, it does possess a Leu-Ile sequence (residues 392 and 393; see Figure 1d) in a potential helix-forming region (LIHRLEAVQR, where the underlined residues are predicted to interact with GSK-3 based on the alignment in Figure 1d). Smalley et al., 1999 [12] found that a mutation (L521P) equivalent to L392P in mouse Axin abolished binding to GSK-3, and Webster et al., 2000 [32] identified a L396M mutation in three human cancer-derived cell lines that interfered with Axin's ability to bind GSK-3. The effect of mutating these residues on the binding of GID to GSK-3 is shown in Table 1. The mutation of Leu 392 or Leu 396 to Met lowered, but did not abolish, the binding of GID to GSK-3, consistent with these residues being on the hydrophobic face of a helix interacting with GSK-3. The mutation of Leu 392 to proline abolished the binding of GID to GSK-3, consistent with the side-chain hydroxyl of Tyr 288 from GSK-3 forming a hydrogen bond to the main-chain amide of Leu 392 (as observed in the GSK-3-FRATtide complex between Tyr 288 and Leu 212; see Figure 3). To conclude, the data are consistent with residues 393–401 of Axin forming an ampipathic α helix that binds to GSK-3 in manner similar, but not identical, to that of the α2 helix on FRATtide. The sequence alignment in Figure 1d suggests that GID would not possess an α1 helix similar to that on FRATtide. While the footprint of Axin on GSK-3 overlaps with that of FRATtide, it is unlikely to be identical. Yuan et al., 1999 [30] have shown that a Y216F mutant of GSK-3β still binds FRAT but has a reduced affinity for Axin, suggesting that Axin may interact directly with TyrP 216.

Discussion

Phosphorylation of residues within the activation loop is a common mechanism for regulating the activity of kinases [23]. In the MAP kinase ERK2, two sites on the activation loop, Thr 183 and Tyr 185, need to be phosphorylated for maximum activity [27]. In GSK-3, the binding sites for both phosphate groups are conserved, and phosphotyrosine 216 in GSK-3 is structurally equivalent to phosphotyrosine 185 in ERK2. However, the residue equivalent to Thr 183 (in ERK2) is Val 214, and the phosphate binding site adjacent to this residue is used in GSK-3 for recognizing the priming phosphorylation on the substrate or the PKB inhibitory phosphorylation site at the amino terminus of GSK-3 [6, 21, 22]. The substitution of a valine for the phosphothreonine seems to have slightly lowered the bottom lip of the substrate binding groove in GSK-3 (compared to ERK2; see Figure 2). Recently published structures of unphosphorylated GSK-3 have a phosphate ion [21] or sulphonate moiety [22] at the primed binding site and have thus suggested that the binding of phosphorylated substrates to GSK-3 may help to induce an active conformation in the activation loop. The conformation of the activation loop we observe in the absence of a sulfate ion at the primed site (crystal form A) is almost identical to that observed in the presence of a sulfate ion, suggesting that phosphorylation of tyrosine 216 is sufficient to induce the correct conformation in the activation loop (residues 220–226 in GSK-3). The crystal structure of the phosphorylated form of GSK-3 therefore suggests that tyrosine 216 phosphorylation may be critical for regulating activity against non-primed substrates.

Studies of the activity of a Y216F mutation of GSK-3 have suggested that the substitution of phenylanine for tyrosine 216 lowers activity some 5- to 10-fold [29, 30]. However, these studies did not distinguish between primed and non-primed substrates, and the Tyr 216 form of the enzyme was not necessarily fully phosphorylated. Although in *Dictyostelium* the tyrosine kinase ZAK1 activates GSK-3 to direct cell fate specification [33], the regulatory role of Tyr 216 phosphorylation in signaling in mammalian cells is less clear. The main method by which insulin inhibits GSK-3 activity is by the phosphorylation of serine 9 by PKB [4, 34], but tyrosine dephosphorylation of GSK-3 may also play a role in response to extracellular signals [35]. Nerve growth factor (NGF) withdrawal from PC12 cells led to increased phosphorylation at Tyr 216, GSK-3β activity, and cell death [36]. This increased cell death may have been at least partially due to enhanced phosphorylation and degradation of β-catenin by GSK-3. Crowder and Freeman [37] have shown that expression of FRAT1 rescues neurons from cell death induced by the inhibition of PI-3 kinase or PKB, but not from cell death caused by NGF withdrawal. Culbert et al. [31] have recently shown that FRAT1 overexpression in PC12 cells is neuroprotective and inhibits phosphorylation of tau and β-catenin but that FRAT1 overexpression is a less-potent method of neuroprotection than ATP-competitive inhibitors of GSK-3. Overexpression of FRAT1 did not inhibit activity toward GS [31].

The FRATtide peptide adopts a helix-turn-helix conformation and, in packing against the C-terminal lobe of GSK-3, induces a change in conformation of a loop in the region between helices G and H. Members of the CDK2, Erk (MAP), Clk, and GSK-3 kinase families all have a large insertion (compared to those of other kinases [26]) in their amino acid sequences in this region, and here we show this region to be functionally significant in GSK-3. In particular the side-chain functions of Tyr 288 and Glu 290 from GSK-3 recognize the largely buried N-terminal end of the second α helix (sequence LIKE) of FRATtide. Mutation of the KE sequence to AQ in the *Xenopus* FRAT homolog, GBP, greatly reduced binding to *Xenopus* GSK-3 [15], although binding of this mutant to GSK-3 could be detected in the presence of *Xenopus* Dsh [16]. While Lys 214 from the LIKE sequence makes a direct interaction with GSK-3 (Figure 3c), the side chain of Glu 215 does not interact directly with GSK-3 but stabilizes the helical conformation of FRATtide by interacting with Arg 218 and Arg 219 one turn down the α2 helix. One model for the function of FRAT in Wnt signaling is that it displaces the scaffold

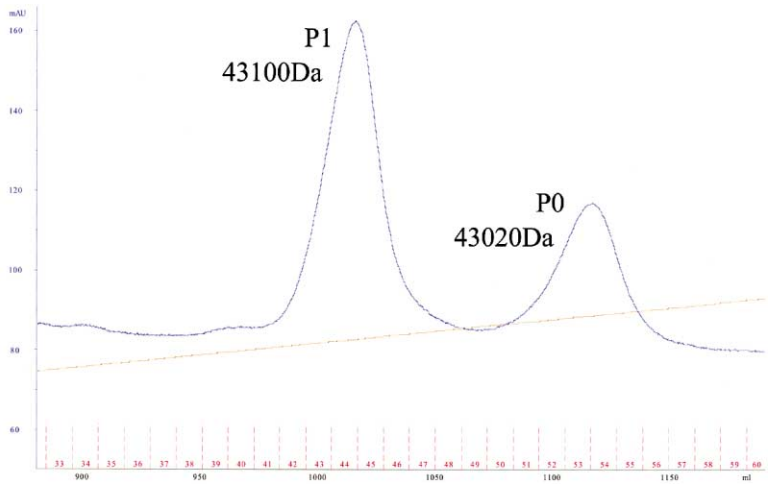

Figure 4. Source 15S Elution Profile

Source 15S elution profile showing separation of the phosphorylated and nonphosphorylated forms of GSK-3β (see Experimental Procedures for details).

protein Axin from GSK-3 and thus inhibits GSK-3 from phosphorylating β-catenin. Consistent with this model is the observation that the Axin-derived peptide GID competes with FRATtide for binding to GSK-3 [31]. Mutations in GID (Table 1) that lower its affinity for GSK-3 are consistent with the hypothesis that the sequence 392-LIHRLEAVQR-401 forms an amphipathic helix that binds to GSK-3 at a site similar to that in FRATtide. The L392P mutation abolishes binding of GID to GSK-3 (Table 1), and this mutation in mouse Axin (L521P) inhibits GSK-3 binding in cellular assays [12].

Potent and selective ATP-competitive inhibitors of GSK-3 [38] stimulate glycogen synthesis in human liver cells and induce the expression of a β-catenin-LEF/TCF-regulated reporter gene in HEK293 cells [24]. These small-molecule inhibitors protect primary neurones from cell death induced by reduced PI-3 kinase pathway activity [25]. The elucidation of the crystal structure of tyrosine 216-phosphorylated GSK-3 bound to FRATtide and a sulfate ion allows us to structurally dissect different ways in which GSK-3 function can be regulated. Small-molecule inhibitors that occupied the sulfate binding site would have the potential to inhibit GSK-3 activity against primed substrates such as glycogen synthase, and small-molecule mimetics of FRATtide may be neuroprotective. At least three regulatory genes in the Wnt signaling pathway are mutated in primary human cancers [39]. Molecules that bound to FRAT and prevented FRAT from displacing Axin on GSK-3 would inhibit Wnt pathways that signal via FRAT-mediated displacement of Axin and could potentially be useful in some human cancers.

Biological Implications

Glycogen synthase kinase-3β is inhibited in response to insulin signaling when it is phosphorylated by PKB on serine 9. The exact mechanism(s) by which GSK-3 activity toward β-catenin is inhibited in Wnt signaling pathways is less clear, but it may involve the GSK-3 binding protein FRAT1.

The crystal structures of uncomplexed Tyr 216-phos-

Table 2. Crystallographic Data and Refinement Statistics

Crystal Form	A, Native phospho-GSK-3β	FS, FRATtide phospho-GSK-3β
Data Collection		
Space group	$P2_1$	R32
Cell a, b, c (Å)	67.6, 115.4, 67.7 (β = 101.98°)	153.1, 153.1, 213.4
Maximal resolution	2.89 Å	2.60 Å
Total/unique reflections	32,874/17,737	333,047/29,716
Completeness	78%	99.9%
R_{sym}[a] (%)	6.7% (20.1%)	6.6% (44.8%)
Refinement		
Protein atoms	5,550	6,059
Residues	696	755
Other atoms	21 (5 H_2O)	168 (140 H_2O, 3 SO_4^{2-}, 1 Tris)
R_{cryst}/R_{free}[2] (%)	21.9%/29.1%	19.6%/26.2%
rmsd bond lengths (Å)	0.013	0.007
rmsd bond angles (degrees)	2.1	1.3

[a] $R_{sym} = \Sigma|I_i - \langle I\rangle|/\Sigma I_i$, where I_i is the intensity of the ith observation of a reflection and $\langle I\rangle$ is the mean intensity of the reflection.
[2] $R_{cryst} = \Sigma||F_{obs} - |F_{cal}||/\Sigma|F_{obs}|$, where $|F_{obs}|$ and $|F_{cal}|$ are the observed and calculated structure factor amplitudes for a reflection. R_{free} was calculated from a disjoint set of reflections (8% of total form A, 5% form FS) selected in thin resolution shells (to avoid possible bias due to NCS in each crystal form).

phorylated GSK-3β and its complex with a peptide and a sulfate ion provide a structural explanation for three ways in which GSK-3 activity can be regulated. Phosphorylation of tyrosine 216 causes the activation loop of GSK-3 to adopt an active conformation and defines the P1 specificty pocket for substrates. The binding of GSK-3 substrates containing a primed phosphoserine residue also seems to promote an active conformation of the activation loop and may help to promote the correct orientation of the N- and C-terminal lobes of the kinase domain for catalysis. Upon phosphorylation by PKB, serine 9 at the N terminus of GSK-3 will occupy the primed binding site, with the N-terminal residues of GSK-3 then blocking its own active site as a pseudosubstrate.

The FRATtide peptide forms two α helices, which bind to the C-terminal lobe of the kinase domain adjacent to, but not obstructing, the substrate access channel. FRATtide competes with Axin for binding to GSK-3, and the footprint of Axin on GSK-3 is expected to be similar to that of FRATtide. A predicted amphipathic helix in Axin may bind to GSK-3 in a similar manner to the second helix of FRATtide. The structure of the GSK-3/FRATtide complex helps to explain how Axin can function as a scaffolding protein that brings GSK-3 and β-catenin together. The GSK-3/FRATtide structure provides an explanation as to why FRATtide does not inhibit GSK-3 from phosphorylating glycogen synthase but does inhibit GSK-3 from binding Axin (and phosphorylating β-catenin). The structure can be used as a template in structure-based drug design for designing inhibitors that inhibit or activate GSK-3 toward specific classes of substrates, which may be associated with disease states such as diabetes, neurodegenerative disease, or cancers.

Experimental Procedures

Expression and Purification

A construct corresponding to residues 27–393 of GSK-3β was designed based on sequence conservation and expressed with an N-terminal deca-His in Sf9 cells (cells were grown and infected with recombinant baculovirus as described previously [40]). Frozen cells were defrosted in buffer A (10 mM MOPS [pH 7.0], 300 mM NaCl, 10% glycerol, 10 mM β-mercaptoethanol, 50 mM NaF, 1 mM Na orthovanadate, 1 mM benzamidine, 1 mM PMSF, 1 μg/ml bestatin, 1 μg/ml lepeptin, 1 μg/ml aprotinin) and disrupted by dounce homogenization, on ice. Cell debris was removed by centrifugation (48,000 g for 60 min at 4°C), and the supernatent was contacted with 10 ml of NiNTA Supreflow (QIAGEN) for 4 hr at 4°C. NiNTA beads were recovered by centrifugation (2000 g for 10 min at 4°C), packed into an XK16 column (Amersham Pharmacia), and washed with 10 Bv (Bed volumes) buffer A, 10 Bv buffer A + 1 M NaCl, and 20 Bv buffer A + 100 mM imidazole before they were eluted with 20 Bv buffer A + 500 mM imidazole on an AKTA Purifier 100 (Amersham Pharmacia). Fractions were analyzed with the Bradford assay (Pierce) and reducing SDS PAGE (Novex).

Cation exchange was performed with Source 15S (Amersham Pharmacia). Fractions from the immobilized metal ion affinity chromatography were pooled, and the buffer was exchanged for buffer B (20 mM MOPS [pH 7.0], 50 mM NaCl, 1 mM DTT, 10% glycerol, 1 mM Na orthovanadate, 1 mM benzamidine, 0.2 mM PMSF) by the use of G25M (Amersham Pharmacia). The fractions were then loaded onto an 8 ml Source 15S column, HR10 (Amersham Pharmacia). This was washed with 5 Bv of buffer B before being eluted with a linear NaCl gradient of 0–500 mM over 50 Bv, 500–1000 mM NaCl over 5 Bv, and 1000 mM at 5 Bv. Five milliliter fractions were collected at 150 cm^{h-1} with an AKTA purifier 100 (Figure 4). Analysis of two peaks from the cation exchange column by electrospray Liquid Chromatography-Mass Spectroscopy (Water 2690 HPLC; Polymer Labs PLRP-S, 300A, 5 μm, 150 × 2.1 mm, H_2O:ACN gradient 15%–75% over 24 min with 0.05% TFA; Micromass LC-T) revealed a mass difference of 80 Da, corresponding to a phosphate ion.

Crystallization of the Phosphorylated Form without and with FRATtide

Initial crystallization experiments gave crystals with the phosphorylated, but not with the unphosphorylated, GSK-3-β protein. The purified protein (concentration up to 4 mg/ml) was crystallized by the hanging-drop vapor diffusion method against wells containing 100 mM Tris Acetate (pH 8.2), 125 mM NaCl, and 6%–14% PEG 8000 (temperature, 277 K). This gave crystal form A (Table 2), which yielded a 2.9 Å data set at EH2 on beamline ID14 at the ESRF (European Synchrotron Radiation Facility, Grenoble); crystals were frozen by serial transfer to 20% glycerol.

Incubation of 39mer peptide FRATtide (0.2–2 mg/ml; purchased from California Peptide Research) with phosphorylated GSK-3β (1–4 mg/ml) improved the solubility of the protein and gave crystals in space group R32 (Table 2; crystal form FS, crystallized from 1.4–2.2 M ammonium sulfate [pH 7–8] with 100 mM Tris or Hepes buffer at room temperature). These crystals were frozen by serial transfer to 25% ethylene glycol (+ crystallization buffer).

Structure Solution and Refinement

X-ray data were collected at EH2 of ID14 at the ESRF, Grenoble. Data from crystal form A (space group $P2_1$) were somewhat anisotropic, and each image was processed with MOSFLM [41] to a resolution at which I/sigmal > 2.5. This gave a data set that was more than 90% complete in most resolution shells but less complete at high resolution. Diffraction data from crystal form FS (FRATtide crystal form, space group R32) were not noticeably anisotropic; the high R_{sym} in the high-resolution shell for this data set (44.8%; Table 2) is probably due to the high redundancy (11.2), and these data were useful in refinement (R_{cryst}/R_{free} = 29.1%/32.2% for the high-resolution shell data at end of refinement). Diffraction data (purified from Sf9 cells) that were collected from SeMet-labeled GSK-3β and cocrystallized with FRATtide were disappointing (3.3 Å) and were not used in the structure determination.

The positions of the two molecules in the asymmetric unit of crystal form A (space group $P2_1$) were located by molecular replacement; coordinates of doubly phosphorylated ERK2 were used as a search model (PDB code 2ERK [27]). The rotation function, calculated with Amore [42], gave clear solutions to the rotation function and translation function peaks above noise. The molecular replacement solution was consistent with the noncrystallographic 2-fold axis, perpendicular to the crystallographic 2_1, which was clearly evident in the self-rotation function (and in the diffraction pattern). After three rounds of refinement with CNX [43] in crystal form A, the R factor (R_{free}) had decreased to 35.5% (42.4%) on data to 2.9 Å (maps were averaged around the noncrystallographic 2-fold axis with the RAVE suite [44]).

Crystal form FS (with FRATtide, space group R32) was solved by molecular replacement with coordinates from crystal form A (after three rounds of refinement), which gave a clear solution (note that the two molecules in R32 gave rise to a single peak in the rotation function). The R32 solution had an initial R factor (R_{free}) of 41.7% (46.7%) on data to 2.8 Å after rigid-body refinement in CNX. Seven rounds of refinement in the R32 crystal form (interspersed with rebuilds on the graphics with XTALVIEW [45]) reduced the R factor (R_{free}) to 24.8% (28.8%) on data to 2.6 Å. These refined coordinates for GSK-3β were transformed back to crystal form A, for which initial rigid-body refinement gave an R factor (R_{free}) of 27.4% (31.6%). Further refinement gave statistics as shown in Table 2. The final structure for crystal form FS shows only two residues from the Ramachandran plot in disallowed regions; these are both cysteine 218 (from molecules A and B). In ERK2 the residue that is equivalent to cysteine 218, Ala 187, has a left-handed conformation ($\phi = 70°$, $\psi = 158°$ [27]); similar conformations for this residue are observed in active CDK2 [28] and in our GSK-3 structure.

Model of Substrate Peptide GSK-3 Complex

The crystal structure of the phosphorylated CDK2/cyclin A/substrate peptide/ATP analog complex (PDB code 1QMZ [28]) was superposed on molecule A of the FS crystal form of GSK-3β (see Figure 2). The substrate peptide (sequence HHASPRK)in the CDK2 active site was then used as a template for modeling a portion of the glycogen synthase substrate, sequence RHSSPHQSp (where Sp represents a phosphoserine) according to the following alignment:

CDK2	substrate	HHASPRK
GSK-3	substrate	RHSSPHQSp

The terminal lysine residue in the CDK2 substrate peptide interacts with the phosphate of phosphothreonine 160 in CDK2; the terminal phosphate of the phosphoserine residue in the GSK-3 substrate was positioned to superpose on the sulfate ion in the GSK-3 crystal structure and thus occupied a similar position to the phosphate on phosphothreonine 160 in CDK2. The resulting model of GSK-3β + substrate peptide (minus sulfate ion) is shown in Figure 2c.

Fluorescence Binding Assay for FRATtide Antagonists

The affinities of GID mutants (Table 1) were assessed with a fluorescently labeled (TAMRA) FRATtide ligand displacement assay as described [31].

Acknowledgments

The authors would like to thank Dave Tolson and Andy West (Mass spectrometry), Ed Mitchell (ESRF, data collection), Martin Saunders (construct design), and Julie Holder, Darren Cross, and Matthew Coghlan for discussion.

Received: July 26, 2001
Revised: October 10, 2001
Accepted: October 18, 2001

References

1. Embin, N., Rylatt, D.B., and Cohen, P. (1980). Glycogen synthase kinase-3 from rabbit skeletal muscle. Seperation from cyclic-AMP-dependent protein kinase and phosphorylase kinase. Eur. J. Biochem. *107*, 519–527.
2. Welsh, G.I., Wilson, C., and Proud, C.G. (1996). GSK3: a SHAGGY frog story. Trends Cell. Biol. *6*, 274–279.
3. Cohen, P. (1999). Identification of a protein kinase cascade of major importance in insulin transduction. Phil. Trans. R. Soc. Lond. B *354*, 485–495.
4. Cross, D.E.A., Alessi, D.R., Cohen, P., Andjelkovich, M., and Hemmings, B.A. (1995). Inhibition of glycogen sythase kinase-3 by insulin mediated by protein kinase B. Nature *378*, 785–789.
5. Welsh, G.I., Miller, C.M., Loughlin, A.J., Price, N.T., and Proud, C.G. (1998). Regulation of eukaryotic initiation factor eIF2B: glycogen sythase kinase-3 phosphorylates a conserved serine which undergoes dephosphorylation in response to insulin. FEBS Lett. *421*, 125–130.
6. Frame, S., Cohen, P., and Biondi, R.M. (2001). A common phosphate binding site explains the unique specificity of GSK3 and its inactivation by phosphorylation. Mol. Cell. *7*, 1321–1327.
7. Cadigan, K.M., and Nusse, R. (1997). Wnt signaling: a common theme in animal development. Genes Dev. *11*, 3286–3305.
8. Miller, J.R., Hocking, A.M., Brown, J.D., and Moon, R.T. (1999). Mechanism and function of signal transduction by the Wnt/β-catenin and Wnt/Ca^{2+} pathways. Oncogene *18*, 7860–7872.
9. Peifer, M., and Polakis, P. (2000). Wnt signaling in oncogenesis and embryogenesis—a look outside the nucleus. Science *287*, 1606–1609.
10. Ikeda, S., Kishida, S., Yamamoto, H., Murai, H., Koyama, S., and Kikuchi, A. (1998). Axin, a negative regulator of the Wnt signaling pathway, forms a complex with GSK-3β and β-catenin and promotes GSK-3β-dependent phosphorylation of β-catenin. EMBO J. *17*, 1371–1384.
11. Hart, M.J., de los Santos, R., Albert, I.N., Rubinfeld, B., and Polakis, P. (1998). Downregulation of β-catenin by human Axin and its association with the APC tumor suppressor, β-catenin and GSK3β. Curr. Biol. *8*, 573–581.
12. Smalley, M.J., et al., and Dale, T.C. (1999). Interaction of Axin and Dvl-2 proteins regulating Dvl-2 stimluated TCF-dependent transcription. EMBO J. *18*, 2823–2835.
13. Sakanaka, C., Weiss, J.B., and Williams, L.T. (1998). Bridging of β-catenin and glycogen synthase kinase-3β by Axin and inhibition of β-catenin-meditated transcription. Proc. Nat. Acad. Sci. USA. *95*, 3020–3023.
14. Jonkers, J., Korswagen, H.C., Acton, D., Breuer, M., and Berns, A. (1997). Activation of a novel proto-oncogene, FRAT1, contributes to progression of mouse T-cell lymphomas. EMBO J. *16*, 441–450.
15. Yost, C., Farr, G.H. III, Pierce, S.B., Ferkey, D.M., Chen, M.M., and Kimelman, D. (1998). GBP, an inhibitor of GSK-3, is implicated in *Xenopus* development and oncogensis. Cell *93*, 1031–1041.
16. Li, L., et al., and Wu, D. (1999). Axin and FRAT1 interact with Dvl and GSK, bridging Dvl to GSK in Wnt-meditated regulation of LEF-1. EMBO J. *18*, 4233–4240.
17. Hsu, W., Zeng, L., and Costantini, F. (1999). Identification of a domain of Axin that binds to the serine/threonine protein phosphatase 2A and a self-binding domain. J. Biol. Chem. *274*, 3439–3445.
18. Willert, K., Shibamoto, S., and Nusse, R. (1999). Wnt-induced dephosphorylation of Axin releases β-catenin from the Axin complex. Genes Dev. *13*, 1768–1773.
19. Thomas, G.M., Frame, S., Goedert, M., Nathke, I., Polakis, P., and Cohen, P. (1999). A GSK3-binding peptide from FRAT selectively inhibits the GSK3-catalysed phosphorylation of Axin and β-catenin. FEBS Lett. *458*, 247–251.
20. Hedgepeth, C.M., Deardorf, M.A., Rankin, K., and Klein, P.S. (1999). Regulation of Glycogen Synthase Kinase 3β and downstream Wnt signaling by Axin. Mol. Cell. Biol. *19*, 7147–7157.
21. ter Haar, E., Coll, J.T., Austen, D.A., Hsiao, H.M., Swenson, L., and Jain, J. (2001). Structure of GSK3β reveals a primed phosphorylation mechanism. Nat. Struc. Biol. *8*, 593–596.
22. Dajani, R., et al., and Pearl, L.H. (2001). Crystal structure of glycogen synthase kinase 3β: structural basis for phosphate-primed substrate specificity and autoinhibition. Cell *105*, 721–732.
23. Johnson, L.N., Noble, M.E.M., and Owen, D.J. (1996). Active and inactive kinases: structural basis for regulation. Cell *85*, 149–158.
24. Coghlan, M.P., et al., and Holder, J.C. (2000). Selective small molecule inhibitors of glycogen synthase kinase-3 modulate glycogen metabolism and gene transcription. Chem. Biol. *7*, 793–803.
25. Cross, D.A.E., Culbert, A.A., Chalmers, K.A., Facci, L., Skaper, S.D., and Reith, A.D. (2001). Selective small-molecule inhibitors of glycogen synthase kinase-3 activity protect primary neurones from death. J. Neurochem. *76*, 1–10.
26. Hanks, S.K., and Hunter, T. (1995). The eukaryotic protein kinase superfamily: kinase (catalytic) domain structure and classification. FASEB J. *9*, 576–596.
27. Canagarajah, B.J., Khokhlatchev, A., Cobb, M.H., and Goldsmith, E.J. (1997). Activation mechanism of the MAP kinase ERK2 by dual phosphorylation. Cell *90*, 859–869.
28. Brown, N.R., Noble, M.E.M., Endicott, J.A., and Johnson, L.N. (1999). The structural basis for specificity of substrate and recruitment peptides for cyclin-dependent kinases. Nat. Cell Biol. *1*, 438–443.
29. Hughes, K., Nikolakaki, E., Plyte, S.E., Totty, N.F., and Woodgett, J.R. (1993). Modulation of the glycogen kinase-3 family by tyrosine phosphorylation. EMBO J. *12*, 803–808.
30. Yuan, H., Mao, J., Li, L., and Wu, D. (1999). Suppression of glycogen synthase kinase activity is not sufficient for leukemia enhancer factor 1 activation. J. Biol. Chem. *274*, 30419–30423.
31. Culbert, A.A., Brown, M.J., Frame, S, Hagen, T., Cross, D.A.E., Bax, B., and Reith, A.D. (2001). GSK-3β inhibition by adenoviral FRAT1 expression in PC12 cells is neuroprotective and induces Tau phosphorylation and β-catenin stabilisation without elevation of glycogen synthase activity. FEBS Lett. *507*, 288–294.
32. Webster, M.-T., et al., and Wooster, R. (2000). Sequence variants of the Axin gene in breast, colon and other cancers: an analysis

of mutations that interfere with GSK3 binding. Genes Chromosomes Cancer *28*, 443–453.
33. Kim, L., Liu, J., and Kimmel, A.R. (1999). The novel tyrosine kinase ZAK1 activates GSK3 to direct cell fate specification. Cell *99*, 399–408.
34. Shaw, M., Cohen, P., and Alessi, D.R. (1997). Further evidence that the inhibition of glycogen synthase by IGF-1 is mediated by PDK1/PKB-induced phosphorylation of Ser 9 and not by dephosphorylation of Tyr 216. FEBS Lett. *416*, 307–311.
35. Murai, H., Okazaki, M., and Kikuchi, A. (1996). Tyrosine dephosphorylation of glycogen synthase kinase-3 is involved in its extracellular signal-dependent inactivation. FEBS Lett. *392*, 153–160.
36. Bhat, R.V., et al., and Lee, C.-M. (2000). Regulation and localization of tyrosine^{216} phosphorylation of glycogen synthase-3β in cellular and animal models of neuronal degeneration. Proc Nat. Acad. Sci. USA *97*, 11074–11079.
37. Crowder, R.J., and Freeman, R.S. (2000). Glycogen synthase kinase-3β activity is critical for neuronal cell death caused by inhibiting phosphatidylinositol 3-kinase or Akt but not death caused by nerve growth factor withdrawal. J. Biol. Chem. *275*, 34266–34271.
38. Smith, D.G., et al., and Ward, R.W. (2001). 3-Anilino-4-arylmaleimides: potent and selective inhibitors of glycogen synthase kinase-3 (GSK-3). Bioorg. Med. Chem. Lett. *11*, 635–639.
39. Polakis, P. (2000). Wnt signaling and cancer. Genes Dev. *14*, 1837–1851.
40. Savopoulos, J.W., et al., and Creasy, C. (2000). Expression, purification, and functional analysis of the human serine protease HtrA2. Protein Expr. Purif. *19*, 227–234.
41. Leslie, A.G.W. (1992). Recent changes to the MOSFLM package for processing film and image plate data. Jnt CCP4/ESF-EACMB Newslett. Protein Crystallogr. *26*.
42. Navaza, J. (1994). AMoRe: an automated package for molecular replacement. Acta Cryst. A *50*, 157–163.
43. Brunger, A.T., et al., and Warren, G.L. (1998). Crystallography & NMR System: a new software suite for macromolecular structure determination. Acta Crystallogr. D *54*, 905–921.
44. Kleywegt, G.J., and Jones, T.A. (1994). Halloween . . . masks and bones. In From First Map to Final Model, S. Bailey, R. Hubbard, and D. Waller, eds. (Warrington, UK: SERC Daresbury Laboratory), pp 59–65.
45. McRee, D.E. (1993). Practical Protein Crystallography (New York: Academic Press).
46. Esnouf, R.M. (1997). An extensively modified version of MolScript that includes greatly enhanced colouring capabilities.
47. Nicholls, A., Sharp, K.A., and Honig, B. (1991). Protein folding and association: insight from the interfacial and thermodynamic properties of hyrdocarbons. Proteins *11*, 281–296.

Accession Numbers

Structure factors and coordinates for the GSK-3β/FRATtide complex have been deposited in the Protein Data Bank and assigned the accession code 1gng.